Liquid Crystals
Publication details, including instructions for authors and subscription information:
http://www.informaworld.com/smpp/title~content=t713926090

The influence of lateral and terminal substitution on the structure of a liquid crystal dendrimer in nematic solution: A computer simulation study

Mark R. Wilson[a]; Lorna M. Stimson[b]; Jaroslav M. Ilnytskyi[c]
[a] Department of Chemistry, University of Durham, Durham DH1 3LE, UK [b] Laboratory of Computational Engineering, Helsinki University of Technology, 02015-HUT, Finland [c] Institute for Condensed Matter Physics, National Acad. Sci. of Ukraine, 79011 Lviv, Ukraine

To cite this Article Wilson, Mark R. , Stimson, Lorna M. and Ilnytskyi, Jaroslav M.(2006) 'The influence of lateral and terminal substitution on the structure of a liquid crystal dendrimer in nematic solution: A computer simulation study', Liquid Crystals, 33: 10, 1167 — 1175
To link to this Article: DOI: 10.1080/02678290600973113
URL: http://dx.doi.org/10.1080/02678290600973113

Liquid Crystals, Vol. 33, No. 10, October 2006, 1167–1175

The influence of lateral and terminal substitution on the structure of a liquid crystal dendrimer in nematic solution: A computer simulation study

MARK R. WILSON*†, LORNA M. STIMSON‡ and JAROSLAV M. ILNYTSKYI§

†Department of Chemistry, University of Durham, South Road, Durham DH1 3LE, UK
‡Laboratory of Computational Engineering, Helsinki University of Technology, P.O. Box 9203, 02015-HUT, Finland
§Institute for Condensed Matter Physics, National Acad. Sci. of Ukraine, 79011 Lviv, Ukraine

(*Received 15 May 2005; accepted 19 July 2006*)

The choice of lateral and terminal substitution can have a major influence on the structure of a liquid crystalline supermolecule, which in turn can induce radically different phase behaviour. In this study we use molecular dynamics simulations to investigate the shape of a liquid crystal dendrimer within a liquid crystalline solvent. A coarse-grained (CG) simulation model is employed to represent a third generation dendrimer in which 32 mesogenic groups are bonded to chains at the end of each branch of the dendrimer. In this CG-model the liquid crystal groups can be appended either terminally or laterally. This bonding option is used to generate the structure of four separate systems: (a) a dendrimer with 32 terminal mesogens, (b) a dendrimer with 32 laterally appended mesogens, (c) and (d) dendrimers with 16 lateral and 16 terminal groups represented with laterally bonded sites on one side of the molecule, model (c) or next to terminally bonded sites, model (d). The simulations show that the dendrimer is able to change shape in response to molecular environment and that the molecular shape adopted depends critically on the nature of the lateral/terminal susbstitution.

1. Introduction

In macromolecular and supermolecular liquid crystals, the orientation of rigid mesogenic groups within the molecule is already known to have profound effects on phase behaviour. For example, in a side chain liquid crystal polymer, changing from terminal to lateral substitution leads to nematics being favoured over smectic mesophases [1–3]. This situation is repeated in liquid crystalline multipedes, where a switch from terminal to lateral substitution also leads to nematic rather than smectic phase formation [4]. However, the influence of lateral and terminal orientations is not always easy to predict and depends crucially on the molecular organization of each part of the molecule in the bulk. In all these cases, a change in molecular shape dramatically influences how molecules can pack, with the change to terminal substitution facilitating a coupling between the bulk structure of the molecule itself and the phase that forms. The influence of shape in liquid crystal supermolecules has been recently summarized in an excellent review by Saez and Goodby [5].

*Corresponding author. Tel: +44 191 334 2144, Fax: +44 191 386 1127. Email: mark.wilson@durham.ac.uk

The preferred structures of liquid crystal supermolecules are quite difficult to probe experimentally. If molecules form smectic or columnar phases, X-ray and neutron diffraction studies provide a mechanism for measurement of layer (or column) spacings. However, this does not always allow the tertiary structure of the molecule itself to be deduced. Moreover, within fluid phases, such as nematics and chiral nematics, even with partial deuteration and neutron diffraction, it is difficult to obtain information about three-dimensional molecular structure. Molecular simulation, at least in principle, provides a means of studying complex stuctures within the framework of a coarse-grained (CG) simulation model. (Here the preferred tool of choice, atomistic simulation, is prohibitively expensive to use because of the difficulty in accessing the systems sizes and time scales needed.) Most recently in this area, CG models have been employed to examine the bulk phase of a side chain liquid crystalline polymer [6] and a model carbosilane dendrimer [7].

In recent work [8] the current authors have simulated a model liquid crystalline dendrimer (LCDr) containing terminally attached mesogens, dissolved in a low molecular mass liquid crystalline solvent. The former consisted of a model carbosilane dendrimer simulated at

Liquid Crystals
ISSN 0267-8292 print/ISSN 1366-5855 online © 2006 Taylor & Francis
http://www.tandf.co.uk/journals
DOI: 10.1080/02678290600973113

a semi-atomistic level in which the main part of the dendrimer was represented by spherical Lennard–Jones sites situated at each heavy atom; and the mesogens (within the dendrimer and representing the solvent) were simulated by means of anisotropic Gay–Berne sites. The simulations demonstrated an interesting coupling between the stucture of the dendrimer and the orientational order of the solvent molecules [8] such that the dendrimer molecule was able to undergo conformational changes to adopt a rod-like shape within a nematic solvent. Rod-shaped structures such as those seen in this study have been suggested as being responsible for the formation of smectic phases of LCDrs [9].

The purpose of the current article is to investigate the role played by terminal and lateral substitution in influencing the structure of such a dendrimer. As shown below, lateral substitution changes the shape of the gas phase structure of the dendrimer. However, it is also expected to influence how the dendrimer changes its molecular structure in response to a change in molecular environment. While this is of interest in itself, it should also be noted that LCDrs can be used in nematic liquid crystal phases (dendrimer-filled nematics) to produce polarizer-free liquid crystal displays [10, 11], which function by controlling light scattering. In this case, application of an electric field causes realignment of nematic domains within the structure, providing switching from a scattering to a transparent mode. Lateral substitution of the dendrimer may be expected to alter significantly the structure of the nematic fluid surrounding the dendrimer.

The arrangement of this paper is as follows: the simulation models used in this work simulation model are described in § 2, results for the structure of the four dendrimers studied in a nematic phase are presented in § 3, and conclusions are drawn in § 4.

2. Simulation model for a liquid crystalline dendrimer

The simulation model used is based on a *simplified structure* for a third generation carbosilane dendrimer. Although, intended as a 'generic model' to study the role of terminal versus lateral substitution, the chemical structure employed closely mimics that of a real terminally substituted dendrimer as synthesized by Shibaev and co-workers [9] (figure 1). In the model,

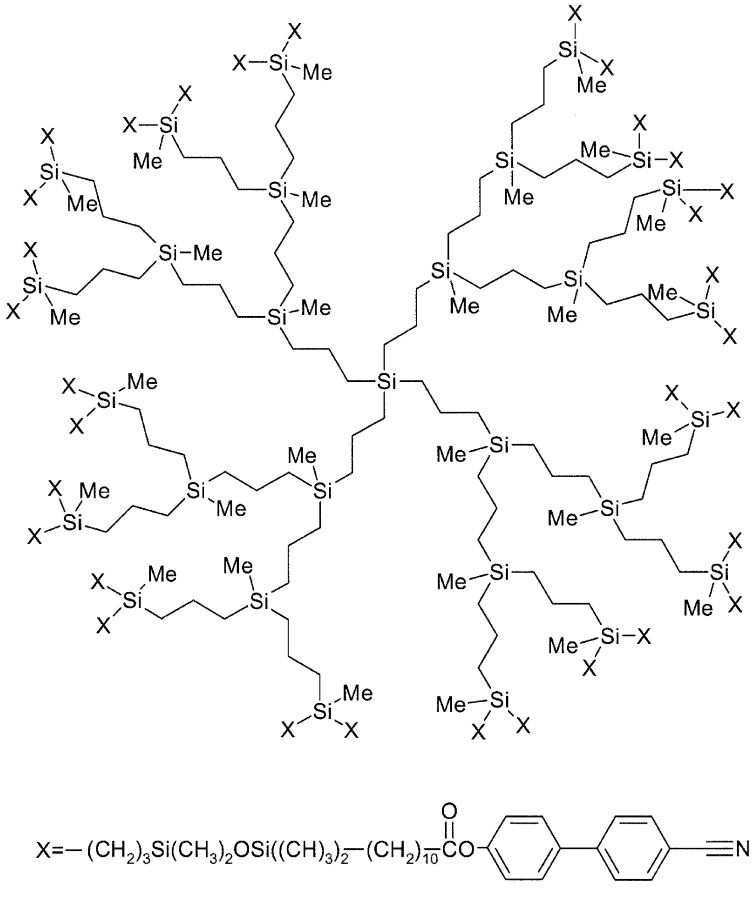

Figure 1. Chemical structure of a third generation carbosilane dendrimer.

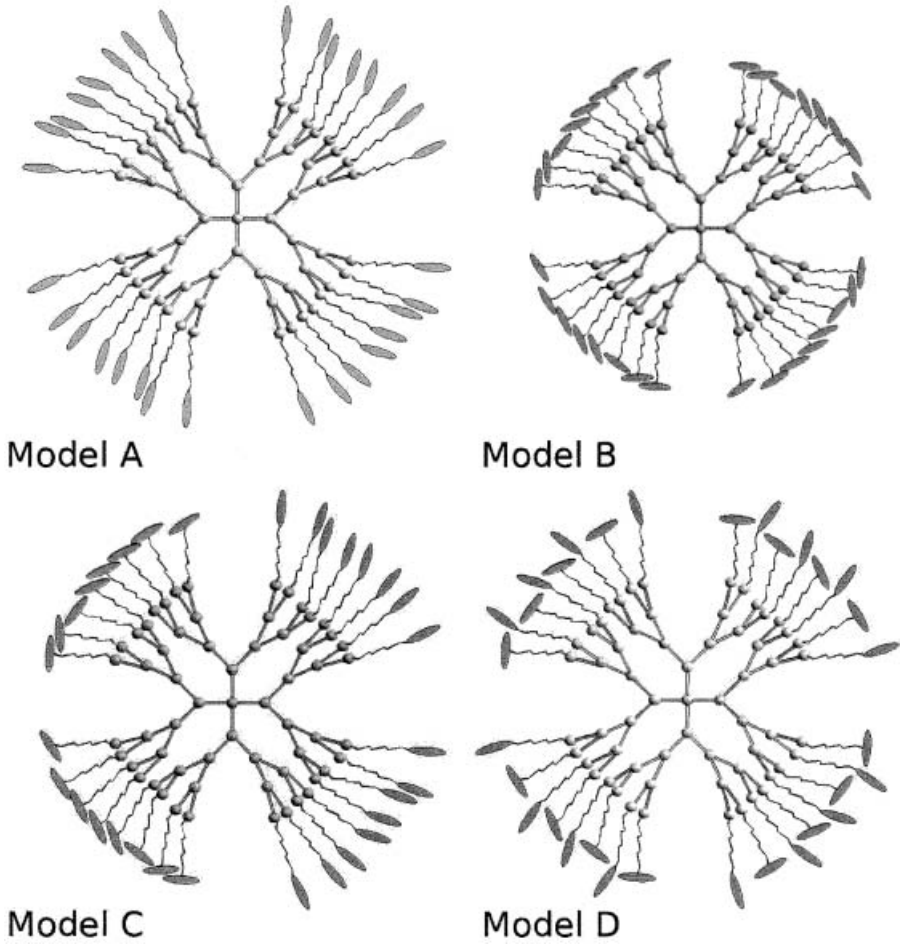

Figure 2. Schematic diagrams showing the branching points, connecting chains and 32 terminal mesogenic groups for the four models A–D. Together, the branching points and connecting chains for each molecule are represented by 781 Lennard–Jones sites.

each heavy atom (silicon, carbon and oxygen) in figure 1 is replaced by a single united atom Lennard–Jones (LJ) site (which incorporates any hydrogens attached to these atom), and the cyanobiphenyl unit plus the ester connecting group are replaced by a Gay–Berne (GB) potential [12]. This gives a total of $N_{\mathrm{LJ}}^{(1)} = 781$ LJ sites and $N_{\mathrm{GB}}^{(1)} = 32$ GB sites in the model dendrimer. This paper simulates four separate dendrimers, with the generic structures shown in figure 2. Model A uses 32 terminally bonded mesogens and was studied initially in a preceeding paper [8]. Model B uses 32 laterally bonded mesogens. Model C uses 16 terminal and 16 lateral mesogens with the lateral mesogens all grouped on one side of the molecule. Model D also uses 16 terminal and 16 lateral mesogens but with laterally and terminally bonded mesogens on adjacent branches as shown. All dendrimers are considered within a liquid crystal solvent.

The building of the initial dendrimer structure required a multi-step process as described in our initial study of model A [8]. In brief, we started from a relaxed molecular structure produced from extensive internal coordinate Monte Carlo calculations [13] of a carefully built atomistic molecular model of figure 1. Hydrogen atoms were removed and each heavy atom was replaced by a single LJ site. In the initial Monte Carlo simulations the mesogenic groups were replaced by rigid rods of Lennard–Jones particles and these were in turn replaced by Gay–Berne particles in the final model. The final stage of preparation involved equilibration in the gas phase using molecular dynamics with the united atom force field described below, immersion in an already equilibrated Gay–Berne nematic phase, then further equilibration over a 4 ns time period. Models B–D were generated by gradually perturbing model A into the required stuctures in the liquid phase. This was achieved by perturbing the equilibrium bond length to the mesogens and the equilibrium 'gb-angle' (see below) to the appropriate ones for each model, over a series of small pertubation steps. These models were then

subjected to further equilibration in the nematic phase over several ns.

The model dendrimers use three types of non-bonded interactions: LJ–LJ, GB–GB and LJ–GB. For the LJ sites, values of $\sigma_{LJ}=3.93$ Å and $\varepsilon_{LJ}/k_B=47$ K (taken from [14]) were used, which are appropriate for a united atom hydrocarbon model, and the cut-off distance for the potential was set to $r_{c,1}=9.8$ Å ($\equiv 2.5\sigma_{LJ}$). For the GB sites we use the cut and shifted form of the potential studied by Brown and coworkers [15], employing a length/breadth ratio $\kappa=3.5$ and a side-to-side/end-to-end well depth ratio of $\kappa'=5$. To scale to real units, values of $\sigma_{GB}=3.829$ Å (estimated from the dimensions of the mesogenic unit) and $\varepsilon_{GB}/k_B=406.15$ K (from [16]) were employed and the cut-off distance was set at $r_{c,2}=22$ Å ($\equiv 5.75\sigma_{GB}$). The extended GB potential [17] was employed to describe the LJ–GB interactions. Here we used $\sigma_{LJ/GB}=\left(\sigma_{GB}^2+\sigma_{LJ}^2\right)^{1/2}\Big/\sqrt{2}\approx 3.88$ A and $\varepsilon_{LJ/GB}=(\varepsilon_{GB}\varepsilon_{LJ})^{1/2}\approx 138.16$ K, with a cut-off distance of $r_{c,3}=16.5$ Å. All non-bonded potentials were shifted at the specified cut-off distances. The three cut-off distances were chosen to give approximately the same maximum numerical error for the potential at the cut-off (the maximum error corresponds to an end-to-end separation in the GB potential and at a point along the GB-axis vector in the LJ–GB interaction).

The intramolecular interactions are described by a simple harmonic force field of the form

$$E_{\text{intra}}=\sum_{\text{bonds}}\frac{k_{\text{bond}}}{2}\left(l-l_{\text{eq}}\right)^2+\sum_{\text{angles}}\frac{k_{\text{angle}}}{2}\left(\theta-\theta_{\text{eq}}\right)^2+\sum_{\text{angles}}\frac{k_{\text{gb}-\text{angle}}}{2}\left(\theta_{\text{gb}}-\theta_{\text{gb}-\text{eq}}\right)^2+\sum_{\text{dihedrals}}\left(a_{0,\text{ dih}}+a_{1,\text{ dih}}\cos\phi+a_{2,\text{ dih}}\cos^2\phi+a_{3,\text{ dih}}\cos^3\phi\right). \quad (1)$$

Here, terms 1,2 and 4 of equation (1) are standard terms in a normal harmonic force field for a united atom system, and the parameters in these terms take their usual meaning [18]. The parameters are fixed by reference to the branched-alkane force field of Vlugt *et al.* [14]. The third term in the force field, the 'gb-angle term' was introduced by Wilson [18, 19] in simulations of liquid crystal dimers. It allows for a Gay–Berne particle to be conveniently bonded to a Lennard–Jones site via the centre of the Gay–Berne, while avoiding free rotation of the latter. θ_{gb} represents the angle between the Gay–Berne long axis and the bond between the Gay–Berne and the Lennard–Jones site. Consequently, the force constant $k_{gb-angle}$ resists deformation of this angle, thereby restricting rotation of the Gay–Berne particle. In molecular dynamics simulations changes to θ_{gb} away from the equilibrium angle θ_{gb-eq} lead to forces on the centres of each site and a restoring torque on the Gay–Berne site. In this work the four models differ only through different values of the angle θ_{gb-eq} and the equilibrium bond length between Gay–Berne and Lennard–Jones particles l_{eq}, as appropriate to terminally and laterally bonded particles. The full set of parameters used in the simulation is summarized in table 1.

The solvent was modelled by GB sites with the same parametrization as those of the LCDr end groups. In this work we used 4441 solvent sites for all the mixture work. The simulations were carried out in the constant-NVT ensemble with a time step of 1 fs using the GBMOL_DD [20, 21] parallel molecular dynamics simulation program. The simulation temperature was $T=400$ K, corresponding to a reduced temperature of $T^*=k_BT/\varepsilon_0^{GB}=0.984$, and the simulations were carried out at a reduced density of $\rho^*=N^*\left(\sigma_0^{GB}\right)^3\Big/V=0.245$. Allowing for the volume of the dendrimer, this corresponds to a nematic phase for our Gay–Berne parameterization, as expected from the work of Brown *et al.* [15] for GB potentials with the same value of $\kappa'=5$ and similar values of κ ($\kappa=3.4$ and $\kappa=3.6$). For convenience we use the same mass and moment of inertia of the solvent GB particles as for those in the dendrimer, this gives a system density in SI units of 1309 kg m^{-3}. For model A we carried out 3 ns of additional simulation beyond the 4 ns performed in the original study. For models B–D all analysis was carried out over run lengths of approximately 6 ns, which followed the equilibration procedure discussed above.

Table 1. Summary of force field parameters used in this study.

Parameter	Value
Mass(GB)	2.9557968×10^{-25} kg
Moment of inertia	0.27305×10^{-23} kg Å^2
Mass(LJ)	0.2324784×10^{-25} kg
$l_{\text{bond}}^{\text{LJ}-\text{LJ}}$	1.53 Å
$l_{\text{bond}}^{\text{LJ}-\text{GB}}$ terminal	7.46 Å
$l_{\text{bond}}^{\text{LJ}-\text{GB}}$ lateral	3.8 Å
k_{bond}	361.291×10^{-20} J Å^{-2}
θ_{eq}	113°
k_{angle}	86.29×10^{-20} J rad^{-2}
$\theta_{\text{gb}-\text{eq}}$ terminal	0°
$\theta_{\text{gb}-\text{eq}}$ lateral	90°
$k_{\text{gb}-\text{angle}}$	86.29×10^{-20} J rad^{-2}
a_0/k_B(non-branched)	1009.728 K
a_1/k_B(non-branched)	2018.466 K
a_2/k_B(non-branched)	136.341 K
a_3/k_B(non-branched)	−3164.52 K
a_0/k_B(branched)	1.394 K
a_1/k_B(branched)	2.787 K
a_2/k_B(branched)	0.188 K
a_3/k_B(branched)	−4.369 K

Each ns required approximately one week of CPU time on AMD Athlon MP processors.

3. Results and discussion

Orientational order in the mixture was monitored by means of four uniaxial order parameters. The general formula

$$S = \langle P_2(\cos\theta_i) \rangle \tag{2}$$

applies to each, where θ_i is the angle between the long axis of the GB particle, $\boldsymbol{e}_i$, and the director. The latter is defined differently for each order parameter. For the total order parameter, S_{mix}, the average in equation (2) is performed over all $N_{\mathrm{GB}}^{(1)} + N_{\mathrm{GB}}^{(2)}$ sites with the director defined globally. S_{den} is measured for dendrimer GB sites only, using their own local director. S_{solv} is defined in the same way but by averaging over solvent GBs. Finally, $S_{\mathrm{d/s}}$ is defined by averaging over all dendrimer GB sites, but measuring θ_i with respect to the director of the solvent. In all cases, measured values of S_{mix} and S_{solv} are almost identical, as the number of mesogens in the solvent outweigh the number in the dendrimer by a factor of $\sim 139\times$, so we quote only the former below.

The order parameter results from the production runs are summarized in figure 3 and the mean values are quoted in table 2. S_{den} and $S_{\mathrm{d/s}}$ are found to very similar in each model. The average values of $S_{\mathrm{d/s}}$ in the table are only 0.02–0.03 smaller than the values for S_{den}, indicating that, in each model, the preferred direction of order of the mesogens is along the director of the nematic solvent. For all models, conformational changes, which allow the dendrimer as a whole to change structure, can allow the mesogens to align on average with the surrounding nematic fluid. Such behaviour has been predicted already by theory [22, 23]. Moreover, it has been postulated in several experimental papers that dendrimers of this type are sufficiently flexible to undergo quite large changes in shape in response to the anisotropy of their environment [24]. The results presented here provide additional support to this view.

During the course of the simulation runs we see quite large fluctuations in the values of S_{den} and $S_{\mathrm{d/s}}$, as a result of large scale conformational rearrangements. The fluctuations are largest for models B and C, where we occasionally see S_{den} and $S_{\mathrm{d/s}}$ dropping to almost zero. We note also that S_{den} and $S_{\mathrm{d/s}}$ for model A are considerably larger than for the other three systems, and the average values for these quantities approach the value of S_{mix}. The reasons for the different behaviour is discussed further below.

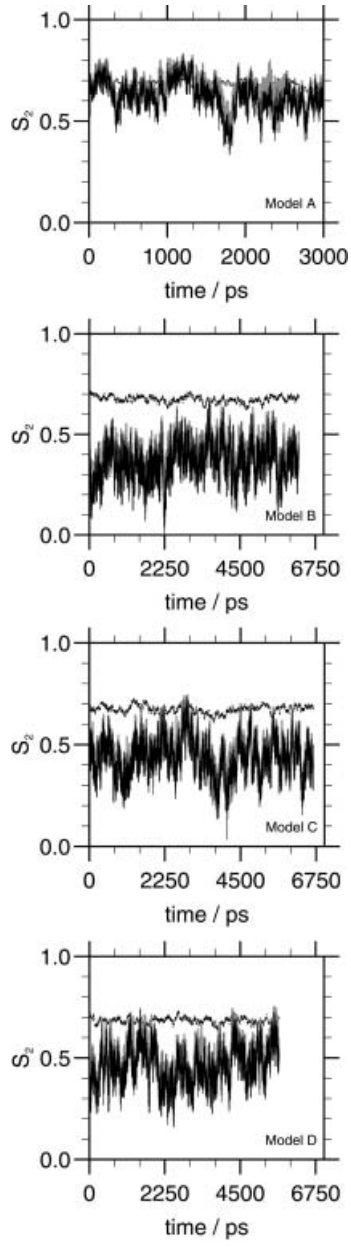

Figure 3. The time dependence of the global system order parameter, S_{mix} (black dotted line); local LCDr order parameter, S_{den} (grey bold line); and the order parameter of the LCDr with respect to the solvent, $S_{\mathrm{d/s}}$ (black bold line) during simulations in a nematic solvent.

The mean dendrimer shape can be assessed by plotting the density distribution parallel, $\rho_{\parallel}(r)$, and perpendicular, $\rho_{\perp}(r)$, to the solvent director. $\rho_{\parallel}(r)$ and $\rho_{\perp}(r)$ are defined within the cone-like sectors limited by the angle $\theta = \pi/6$ around the head and tail directions of the nematic director for $\rho_{\parallel}(r)$, and within the sector with the values for $\theta \in [\pi/3,\ 2\pi/3]$ rad for $\rho_{\perp}(r)$; where θ corresponds to the polar angle in the spherical coordinates with the z-axis ($\theta = 0$) coincident with the

Table 2. Mean and standard deviation of order parameters, S_{den} and $S_{d/s}$ and S_{mix}.

Model	S_{den}	$S_{d/s}$	S_{mix}
A	0.65 ± 0.06	0.62 ± 0.08	0.68 ± 0.01
B	0.39 ± 0.08	0.36 ± 0.09	0.67 ± 0.02
C	0.44 ± 0.08	0.42 ± 0.08	0.68 ± 0.02
D	0.49 ± 0.09	0.46 ± 0.09	0.68 ± 0.01

director. $\rho_{\parallel}(r)$ and $\rho_{\perp}(r)$ are shown for each model in figure 4 and also for model A in the isotropic phase. Here for comparison purposes the mass of the Gay–Berne has been distributed over 11 sites along the long axis of the particle. From figure 4 it is evident that for each model dendrimer, the surrounding nematic phase influences the overall tertiary structure. Changes in the conformation of the alkyl chains allows the dendrimer to become slightly rod-shaped, as witnessed by the difference in the distribution of the outer segments of the dendrimer and the mesogens in parallel and perpendicular directions. This effect is particularly noticable for model A, where $\rho_{\parallel}(r)$ and $\rho_{\perp}(r)$ for the mesogens are very similar in the liquid phase but very little of the density appears within $\rho_{\perp}(r)$ for the nematic phase. Moreover, for all systems, the lines correponding to the mesogenic density extend to longer distances for $\rho_{\parallel}(r)$ in comparison with $\rho_{\perp}(r)$.

The reasons for these differences become apparent if snapshots of configurations from each model are viewed, see figure 5. The mesogenic groups align with the surrounding nematic fluid and this has the effect of perturbing the dendrimer structure overall. For model A, figure 5 (*a*), with wholly terminally bonded mesogens, the dendrimer is able to form a rod with the mesogens excluded to each end of the dendrimer. Here we are obtaining a strong thermodynamic selection of conformations enhancing rod-shaped structures over spheres. This type of rod-shaped structure has been suggested to be responsible for smectic A phase formation in carbosilane dendrimers with terminally bonded mesogenic groups [24]. In such a system, a rod-shaped structure, with mesogens together at the two ends of the molecule, enhances microphase separation in the bulk thereby stabilizing smectic phases.

In contrast to model A, in model B the alkyl chains are unable to rearrange as freely. Here, laterally bonded mesogens can not easily lie at two ends of the dendrimer and still be orientated along the solvent director. Consequently, in model B although the mesogens are able to rearrange to lie along the director, their positions remain distributed over the surface of the dendrimer. In models C and D, with equal numbers of laterally and terminally bonded mesogens, an

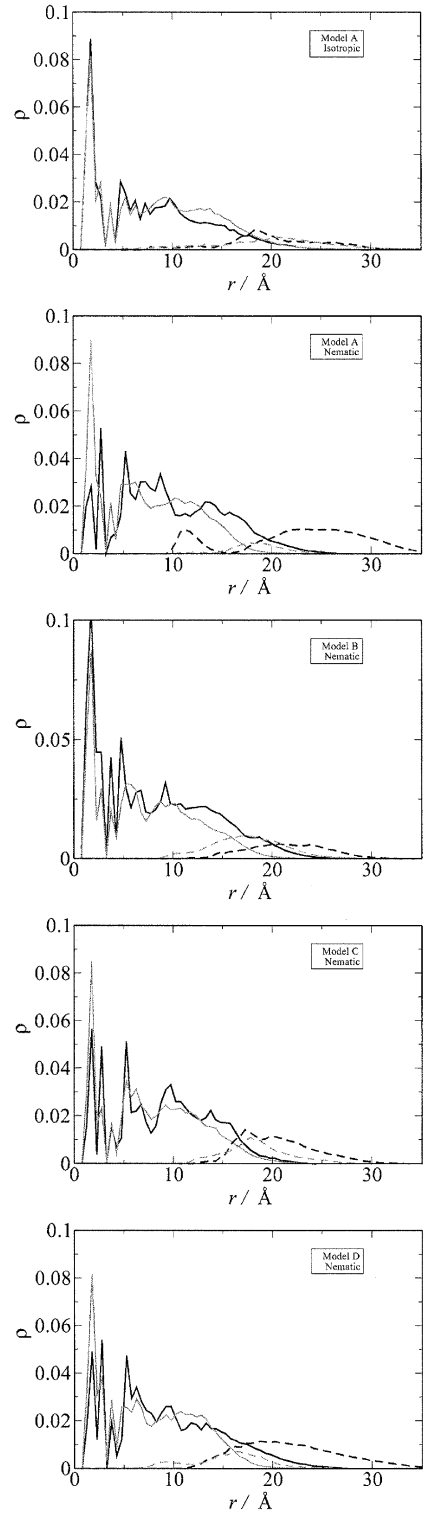

Figure 4. The density distribution functions, $\rho_{\parallel}(r)$ (black lines) and $\rho_{\perp}(r)$ (grey lines), in arbitrary units, for separate parts of the dendrimer for distances measured relative to the central atom in the dendrimer core. Bold line — dendrimer core, dotted line—mesogens.

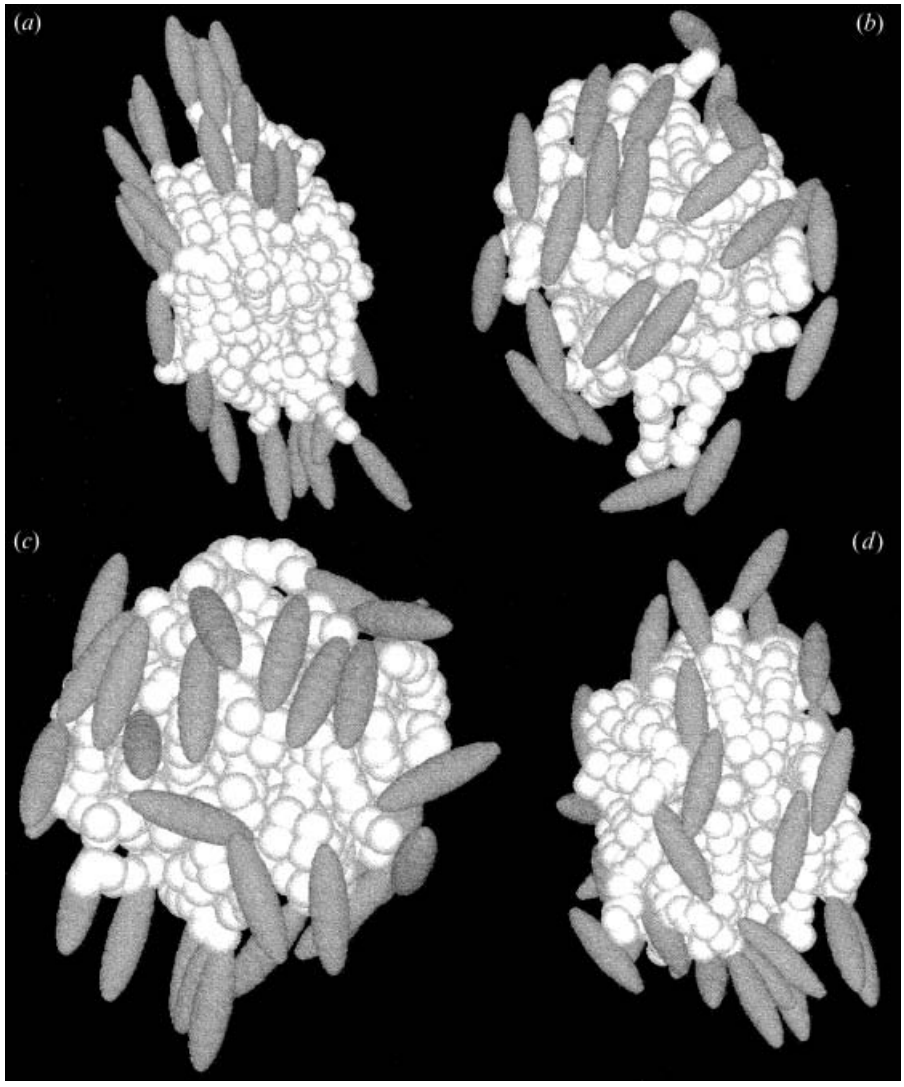

Figure 5. Snapshots taken from simulations of models A–D in the nematic phase. (*a*) Model A; (*b*) model B; (*c*) model C; (*d*) model D. Spherical sites are shown in white and Gay–Berne sites in grey.

intermediate situation is seen. Here, the terminally bonded mesogens migrate to the ends of the dendrimer and the laterally bonded mesogens occupy the surface. Interestingly, it appears to be far easier to achieve this for model D, where terminally and laterally bonded mesogens alternate. In this model there is clearly less steric hindrance and the terminal mesogens can migrate to both ends of the dendrimer. In model C, a Janus-type mesogen, the terminally bonded mesogens must remain on one side of the dendrimer rod. As a consequence of this, the mean values of S_{den} and $S_{\mathrm{d/s}}$ are slightly lower in model C compared with model D.

From both the snapshots and a comparison of $\rho_{\parallel}(r)$ and $\rho_{\perp}(r)$ in figure 4, it is clear that the non-mesogenic parts of the molecule are also perturbed by the presence of the nematic phase. The alkyl chains are extended slightly along the director, with the tail of the density distributions extending by 3–5 Å. It seems likely that the alkyl chains fulfill an important role for liquid crystalline dendrimers in allowing an optimum arrangement of mesogenic units to be adopted. The difference between *gauche* and *trans* conformational energies for an alkyl chain is relatively small, $\approx 4\,\mathrm{kJ\,mol^{-1}}$. Moreover, we know both from theory and from atomistic simulation studies in the nematic phase, that the effective free energy difference between *gauche* and *trans* conformations can be influenced by a nematic mean field [25, 26]. Hence, differences in $\rho_{\parallel}(r)$ and $\rho_{\perp}(r)$ for the chains would be expected, because it should be relatively easy for a nematic fluid to perturb chain conformations sufficiently to allow the molecule to adopt preferential conformations.

Table 3. Principal moments of inertia calculated for each model in a nematic solvent. 'Core' represents the inner 125 atoms of the dendrimer up to the point where chains are connected. 'Core+chains' represents all non-mesogenic sites.

Model	Atoms	$I_{xx}/10^{-21}\,\mathrm{kg\,Å^2}$	$I_{yy}/10^{-21}\,\mathrm{kg\,Å^2}$	$I_{zz}/10^{-21}\,\mathrm{kg\,Å^2}$
A	core	0.10	0.13	0.14
B	core	0.09	0.15	0.16
C	core	0.11	0.13	0.16
D	core	0.08	0.14	0.16
A	core+chains	1.7	2.3	2.6
B	core+chains	1.7	2.3	2.6
C	core+chains	1.9	2.0	2.4
D	core+chains	1.8	2.2	2.4

We have also calculated the principal moments of inertia for the central core (inner 125 atoms) and the core plus Lennard–Jones chains; the results are shown in table 3. As expected from the distribution functions in figure 4, we see deviations from a spherical distribution (the three principal moments are not equal). The main effect is seen for models A and B. For these two systems, and also model D, the eigenvector corresponding to the lowest principal moment for these systems is, on average, along the director. For model C, no strong preference in direction is seen for this eigenvalue (as expected from figure 4), indicating that the differences in I_{xx}, I_{yy}, I_{zz}, seen for this model are the result of conformational fluctuations away from a spherical structure. (Random fluctuations in the structure also occur in the isotropic phase with no preference for the direction of the eigenvector associated with I_{xx}.) Although some distortion of the core itself is seen, its magnitude is small because of the relative rigidity of the central scaffold. Far larger distortions from a spherical distribution are seen for the core plus chains.

We would expect the differences in average structure seen here in solution to be significant for bulk mesophase formation. Here we would expect that a reduction in the rod-like nature of the mesogens, coupled with a reduction in segregation of mesogenic groups to the end of the molecule, would lead to a reduction in stability for smectic mesophases as lateral substitution takes place. In particular, when mesogenic groups are 'scattered over the surface' of a macromolecule, we expect microphase separation to be disrupted.

Finally, we note that a major effect of lateral substitution is to restrict orientational order through steric hindrance. For the terminal chains used here, steric constraints prevent the same degree of alignment that can be achieved with terminally bonded mesogens. Despite the flexibility presented by 16 sites in the chains, there is simply not enough conformational freedom available for all mesogens to align under the influence of the surrounding nematic fluid. It is clear from recent work that this can have important ramifications. Merkel *et al.* [27] have reported studies of a biaxial nematic liquid crystalline tetrapode. Here, four mesogens are bonded laterally to organosiloxane chains which radiate from a central Si atom. Here it seems likely that the biaxiality arises from the combination of two effects, (a) the inability of the chains to provide sufficient conformational freedom for the mesogens to sample orientations uniformly, (b) hindered rotation about the long molecular axis of the mesogens. Both effects are the result of lateral substitution.

4. Conclusions

The effects of lateral and terminal substitution on the structure of a complex macromolecular liquid crystal have been modelled for the first time by molecular simulation. We have carried out molecular dynamics calculations for four model liquid crystalline dendrimers exhibiting different degrees of terminal and lateral substitution of mesogenic units. In the case of a dendrimer with purely terminal substitution, terminal alkyl chains are able to change conformation to allow the mesogenic units to lie parallel to the director at either end of the dendrimer, thereby forming a rod-shaped particle. This is not possible when lateral substitution is employed. Instead mesogenic groups are scattered over the 'surface' of the dendrimer and steric hindrance leads to a reduced orientational order for the mesogenic groups. When a mixture of lateral and terminal substitution is used, the terminally bonded mesogens are able to migrate to the ends of the dendrimer to form partial rods, with the remaining laterally bonded groups scattered over the dendrimer surface. Hence, despite conformational freedom, lateral substitution is found to have a dramatic effect on molecular shape. We expect this change in shape to have a major influence in determining the packing of molecules in the bulk and consequently the mesophases that can form.

Acknowledgments

The authors wish to thank the UK EPSRC for funding High Performance Computers at the University of Durham to carry out this study, and for providing a PDRA for J.M.I. and a Ph.D. studentship for L.M.S.

References

[1] F. Hessel, H. Finkelmann. *Polym. Bull.*, **14**, 375 (1985).
[2] F. Hessel, H. Finkelmann. *Polym. Bull.*, **15**, 349 (1986).
[3] F. Hessel, R.P. Herr, H. Finkelmann. *Makromol. Chem.: macro. Chem. Phys.*, **188**, 1597 (1987).
[4] I.M. Saez, J.W. Goodby. *J. mater. Chem.*, **13**, 2727 (2003).
[5] I.M. Saez, J.W. Goodby. *J. mater. Chem.*, **15**, 26 (2005).
[6] L.M. Stimson, M.R. Wilson. *J. chem. Phys.*, **123**, 034908 (2005).
[7] Z.E. Hughes, M.R. Wilson, L.M. Stimson. *Soft Matter*, **1**, 436 (2005).
[8] M.R. Wilson, J.M. Ilnytskyi, L.M. Stimson. *J. chem. Phys.*, **119**, 3509 (2003).
[9] R.M. Richardson, S.A. Ponomarenko, N.I. Boiko, V.P. Shibaev. *Liq. Cryst.*, **26**, 101 (1999).
[10] M. van Boxtel, D. Broer, C. Bastiaansen, M. Baars, R. Janssen. *Macromol. Symp.*, **154**, 25 (2000).
[11] M.W.P.L. Baars, M.C.W. van Boxtel, C.W.M. Bastiaansen, D.J. Broer, S.H.M. Sontjens, E.W. Meijer. *Adv. Mater.*, **12**, 715 (2000).
[12] J.G. Gay, B.J. Berne. *J. chem. Phys.*, **74**, 3316 (1981).
[13] M. Wilson. *Liq. Cryst.*, **21**, 437 (1996).
[14] T.J.H. Vlugt, R. Krishna, B. Smit. *J. phys. Chem. B*, **103**, 1102 (1999).
[15] J.T. Brown, M.P. Allen, E.M. del Rio, E. de Miguel. *Phys. Rev. E*, **57**, 6685 (1998).
[16] M.R. Wilson. *J. chem. Phys.*, **107**, 8654 (1997).
[17] D.J. Cleaver, C.M. Care, M.P. Allen, M.P. Neal. *Phys. Rev. E*, **54**, 559 (1996).
[18] M.R. Wilson. *J. chem. Phys.*, **107**, 8654 (1997).
[19] C. McBride, M.R. Wilson. *Mol. Phys.*, **97**, 511 (1999).
[20] J.M. Ilnytskyi, M.R. Wilson. *Comput. Phys. Commun.*, **134**, 23 (2001).
[21] J.M. Ilnytskyi, M.R. Wilson. *Comput. Phys. Commun.*, **148**, 43 (2002).
[22] A. Terzis, A. Vanakaras, D. Photinos. *Mol. Cryst. liq. Cryst.*, **330**, 517 (1999).
[23] A.G. Vanakaras, D.J. Photinos. *J. mater. Chem.*, **11**, 2832 (2001).
[24] S.A. Ponomarenko, N.I. Boiko, V.P. Shibaev, R.M. Richardson, I.J. Whitehouse, E.A. Rebrov, A.M. Muzafarov. *Macromolecules*, **33**, 5549 (2000).
[25] J.W. Emsley, G.R. Luckhurst, C.P. Stockley. *Proc. r. Soc. London A*, **381**, 117 (1982).
[26] C. McBride, M.R. Wilson, J.A.K. Howard. *Mol. Phys.*, **93**, 955 (1998).
[27] K. Merkel, A. Kocot, J.K. Vij, R. Korlacki, G.H. Mehl, T. Meyer. *Phy. Rev. Lett.*, **93** (2004).